Absorbing layers for the simulation of open boundaries in TLM field computation

Michel Ney, Sandrick Le Maguer

Absorbing Layers for the Simulation of Open Boundaries in TLM Field Computation

Michel M. Ney and Sandrick Le Maguer
Laboratory for Electronics and Communication Systems (LEST), UMR CNRS 6616
Ecole Nationale Supérieure des Télécommunications de Bretagne, BP 832, 29285 BREST Cedex, FRANCE

Abstract

Like other so-called volumic methods, the TLM requires artificial boundaries when simulations of open problems are performed. There are two cases for which artificial boundaries are needed: when structures under investigation are surrounded by unbounded space or when discontinuity characterization needs matched loads. These artificial boundaries enforce conditions commonly named absorbing boundary conditions (ABC). The paper discusses the most recent techniques based on absorbing media and their implementation in TLM computations.

I. Introduction

The perfect matched layer (PML) technique, originally developed by Bérenger [1] for the FDTD, is currently under intense investigation. It has been found that PML technique is more efficient for inhomogeneous media than one-way equation techniques and, in addition, it is numerically stable and can cope under certain conditions, with evanescent waves. The PML technique is based on the insertion of absorbing layers at the limit of the computational domain. These layers are seen as perfectly matched media by a traveling wave (or transparent for evanescent waves) incident from the computational domain at any angle and for arbitrary frequency. More recently, anisotropic PML media were proposed to enhance the performance with respect to the evanescent waves [2]. Finally, Transparent absorbing boundary (TAB) was proposed for FDTD computation [3]. It consists in multiplying the true field solution by space functions that vanish at the limits of the computational domain. The so-called auxiliary fields are computed using a finite difference scheme. The true values of the fields can be readily computed form the auxiliary fields. The reported performances are as good as the ones obtained with PML techniques. However, this technique does not require extra computations in layers surrounding the domain of interest. It is only recently that absorbing media techniques have been implemented for TLM simulations (see for instance [4, 5]). In this paper, a review of the implementation of the PML in the TLM algorithm is presented and the potential use of anisotropic PML and TAB techniques discussed.

II. Perfectly Matched Layer (PML)

Consider a fictitious medium that has constitutive parameters ε, μ and, electric and magnetic conductivities σ and σ^*, respectively. In such a charge-free homogeneous and isotropic medium, fields are governed by the following curl's Maxwell's equations in the sinusoidal steady-state:

$$\nabla \wedge \boldsymbol{E} = -j\omega\mu \cdot \boldsymbol{H} - \sigma^* \cdot \boldsymbol{H} \qquad (1) \qquad\qquad \nabla \wedge \boldsymbol{H} = j\omega\varepsilon \cdot \boldsymbol{E} + \sigma \cdot \boldsymbol{E} \qquad (2)$$

For a plane wave propagating along, say, the z-axis the wave equation writes:

$$\frac{\partial^2 E_x}{\partial z^2} - (j\omega\mu \cdot + \sigma^*) \cdot (j\omega\varepsilon \cdot + \sigma) E_x = 0 \qquad (3)$$

from which we derive the intrinsic impedance of the medium:

$$\eta = \sqrt{\frac{\mu}{\varepsilon}} \cdot \frac{(1 - j\sigma^*/\omega\mu)^{1/2}}{(1 - j\sigma/\omega\varepsilon)^{1/2}} \qquad (4)$$

Thus, if one has the condition:

$$\frac{\sigma}{\varepsilon} = \frac{\sigma^*}{\mu} = p \qquad (5)$$

then its wave impedance is exactly matched to a medium with intrinsic impedance $\sqrt{\mu/\varepsilon}$. This result holds at any frequency, provided that normal incidence is achieved. The idea of the PML technique is to create a new fictitious layer medium that can be perfectly matched in the three directions of propagation. In such a medium (1) and (2) are

transformed by splitting each field component into two subterms. For instance, one can rewrite (1) and (2) in the time-domain for $E_x=E_{xy}+E_{xz}$ and $H_x=H_{xy}+H_{xz}$, which yields:

$$\mu\frac{\partial H_{xy}}{\partial t}+\sigma_y^* H_{xy}=-\frac{\partial\left(E_{zx}+E_{zy}\right)}{\partial y}=-\frac{\partial E_z}{\partial y} \quad (6) \qquad \mu\frac{\partial H_{xz}}{\partial t}+\sigma_z^* H_{xz}=\frac{\partial\left(E_{yz}+E_{yx}\right)}{\partial z}=\frac{\partial E_y}{\partial z} \quad (7)$$

$$\varepsilon\frac{\partial E_{xy}}{\partial t}+\sigma_y E_{xy}=\frac{\partial(H_{zx}+H_{zy})}{\partial y}=\frac{\partial H_z}{\partial y} \quad (8) \qquad \varepsilon\frac{\partial E_{xz}}{\partial t}+\sigma_z E_{xz}=-\frac{\partial(H_{yz}+H_{yx})}{\partial z}=-\frac{\partial H_y}{\partial z} \quad (9)$$

in which electric and magnetic conductivities pertaining to y and z directions are introduced. Thus a total of 12 equations similar to the above are necessary to simulate a PML medium. For perfect match at any incidence and frequency, conductivities in PML equations have to fulfill (5). Thus, a wave impinging at any incident angle undergoes no reflection, no refraction and is attenuated while traveling in the PML medium. It is also important to note that when considering the interface between PML and a lossless computational domain perpendicular to the ζ-direction, then perfect matching is achieved by considering only $(\sigma_\zeta, \sigma_\zeta^*) \neq 0$ with $\zeta \in \{x,y,z\}$ (uniaxial PML). However, one has to consider all six conductivities for corners limiting the computational box. Also, one can easily show that evanescent waves with direction of attenuation perpendicular to the interface are not distorted by the PML but do not undergo additional attenuation. PML layers are usually terminated by perfectly conducting walls. Finally, tapered conductivities' profile must be used to avoid numerical reflections at the PML interface.

II.1 Interface FDTD-PML/TLM (non unified or split algorithm)

The field subterms are computed via the finite difference form of the PML equations (for example ((6) to (9)). The subterms, for instance E_{xy} and E_{xz}, are defined at the same time and location of their field component they are derived from (E_x in the above exemple). However, it is well known that the field components in the Yee's cell are not defined at the same location as in the TLM-SCN (see fig. 1). Therefore, the only way to interface both algorithms is to proceed to some interpolation. The whole procedure can be decomposed into three steps [6]:

1. Standard algorithms are applied: In the TLM cells adjacent to the interface: $\mathbf{E}^n$, $\mathbf{H}^n$ at the center of the cell, are computed from the known incident voltages at time n-1/2. In the FDTD cells adjacent to interface, $\mathbf{H}^n$-field components normal to the cell faces are computed with the standard Yee's algorithm.
2. Reflected voltages at time n+1/2 are computed via $\mathbf{E}^n$, $\mathbf{H}^n$ and incident voltages at time n-1/2 (accelerated algorithm [7]). $\mathbf{H}^n$-components (in the TLM domain on the faces of the adjacent cells) required by the FDTD to compute $\mathbf{E}^{n+1/2}$ on the interface are interpolated between adjacent TLM cells.
3. Tangential $\mathbf{E}$-components on the interface required by the TLM are interpolated from the FDTD values on the interface. Then, TLM impulses are transferred except at arms normal to the interface where they are computed from the above interpolated tangential $\mathbf{E}$-components and the reflected voltages found in step 2).

Then, a new interpolation procedure can start for the next time iteration. It can be mentioned that only one cell on each side of the interface are involved in the process unlike in [4].

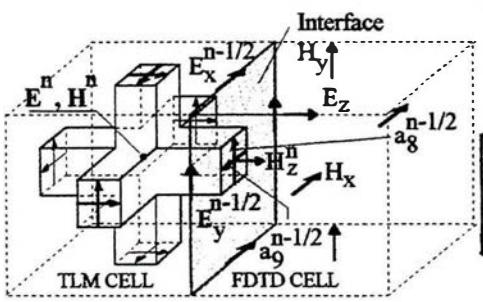

Fig. 1: Interface between a Yee's and a TLM-SCN cell.

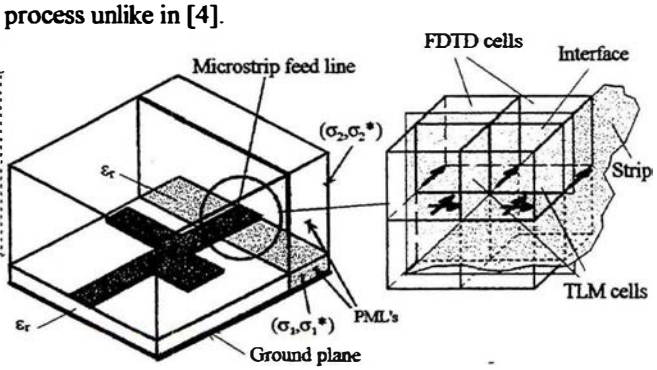

Fig. 2: Conducting strip discontinuity due to the misalignment of electric field components.

The advantage of this approach is the relatively low memory cost of the FDTD algorithm in the PML, the stability and relatively good absorbing performances. The drawback are the additional parasitic reflections at the interface due to the interpolation procedure. This is accentuated when high-field gradients prevails like in the case of the matched

load for a microstrip line illustrated in fig. 2. A refined mesh is required to decrease these reflections as well as the misalignment effect [6].

II.2 Unified TLM-SCN algorithm

Without loss of generality consider the case of uniaxial PML for which only (σ_z, σ_z^*) $\neq 0$ (interface perpendicular to z-axis). First, we shall derive the contribution of subterms to the field component E_x at the center of the cell:

$$\varepsilon_r\varepsilon_0\frac{\partial E_x}{\partial t}+\sigma_z E_x+(-\sigma_z E_{xy})=\frac{\partial H_z}{\partial y}-\frac{\partial H_y}{\partial z} \qquad (10)$$

$$\varepsilon_r\varepsilon_0\frac{\partial E_{xy}}{\partial t}+E_{xy}=\frac{\partial H_z}{\partial y} \qquad (11)$$

$$\varepsilon_r\varepsilon_0\frac{\partial E_x}{\partial t}+\sigma_y E_x+(\sigma_z E_{xz})=\frac{\partial H_z}{\partial y}-\frac{\partial H_y}{\partial z} \qquad (12)$$

$$\varepsilon_r\varepsilon_0\frac{\partial E_{xz}}{\partial t}+\sigma_z E_{xz}=-\frac{\partial H_y}{\partial z} \qquad (13)$$

Comparing with Maxwell-Ampère's law (2), one can identify in (10) and (12) as curl's field equations in homogeneous media which can be simulated by the standard SCN. In addition, one can identify source terms given by the expressions in brackets controlled by field subterms governed by (11) and (13), respectively. Thus, following the procedure described in [8] one can evaluate the value of these controlled source at the center of the TLM cell in terms of incident voltages. To achieve this, one introduces two voltages per subterms that should correctly approximate (11) and (13) (see fig. 3). Among the various possibilities to combine PML equations, the one presented here gave the best results in terms of stability. For uniaxial PML simulation, only 26 voltages are required. For multiaxial PML, the fully loaded TLM node includes 30 voltages. It reduces to 27 and 24 voltages for its hybrid and super condensed version, respectively. The absorbing performance is slightly better than with the split algorithm. However, instability occurrences had to be circumvented by reducing the time step [9]. The procedure to construct a PML-TLM cell is not unique as field samples in the TLM cell can be chosen at different locations. For instance in [10], one sample (voltage) is taken at the center of the cell for the subterms. As a result, only 24 voltages are needed for the SCN. Another scheme was presented in [11] with a circuit approach for the construction of a PML-TLM node. It is difficult to compare absorbing performances between the different schemes as no absorption figures were reported in [10] and [11] but rather error levels in field magnitude for free space propagation simulations.

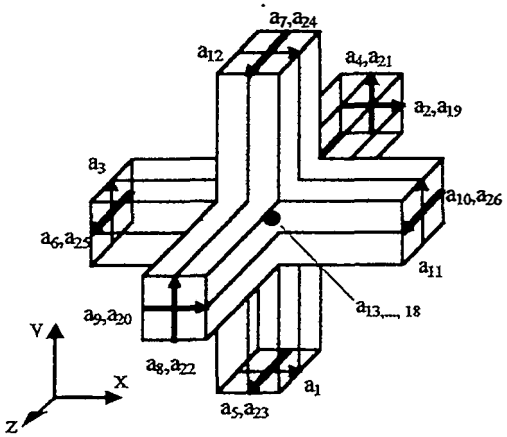

Fig. 3: Voltages in PML-TLM node (uniaxial)

II.3 Anisotropic PML

In order to avoid the manipulation of field subtermes, Gedney [2] proposed to introduce a maxwellian anisotropic medium with diagonal permittivity and permeability tensors. For instance, the Maxwell-Ampère curl's equation is written in sinusoidal steady-state as:

$$\frac{\partial H_k}{\partial j}-\frac{\partial H_j}{\partial k}=j\omega\varepsilon\frac{s_j s_k}{s_i}E_i \qquad i,j,k\in\{x,y,z\} \qquad (14)$$

with $s_i=\alpha_i[1+\sigma_i/(j\omega\varepsilon)]$ where α_i and σ_i correspond to evanescent and traveling waves, respectively. Note that s_i can be chosen arbitrarily. The idea is to write (14) in the time domain, for instance:

$$\frac{\partial H_k}{\partial j}-\frac{\partial H_j}{\partial k}=\frac{s_j s_k}{s_i}\left[\varepsilon\frac{\partial E_i}{\partial t}+(\sigma_k+\sigma_j-\sigma_i)E_i+F_i\right] \qquad (15)$$

$$\varepsilon\frac{\partial F_i}{\partial t}+\sigma_i F_i=\gamma_i E_i \qquad (16)$$

in which $\gamma_i=\left[\sigma_j\sigma_k-\sigma_i(\sigma_k+\sigma_j-\sigma_i)\right]$. Manipulating Faraday-Maxwell's law yields similar equations. To implement the above relations in the TLM algorithm, one follows the general procedure described in [8]. This results in adding six stubs to compute auxiliary quantities at the center of the cell (only two in the uniaxial case). The advantage of the approach is that 24 voltages only are needed for the general case. It reduces to 21 and 18 voltages for the the Hybrid and Symmetrical Super Condensed nodes, respectively.

II.4 Transparent Absorbing Boundary (TAB)

More recently, a procedure based on field mapping was presented [3]. FDTD simulations for free-space propagation showed excellent absorption performances. The idea is to write auxiliary fields in terms of the true solutions $\mathbf{E}_0(\mathbf{r},t)$, $\mathbf{H}_0(\mathbf{r},t)$ as:

$$\mathbf{E}(\mathbf{r},t) = F(\mathbf{r})\,\mathbf{E}_0(\mathbf{r},t) \qquad (17) \qquad\qquad \mathbf{H}(\mathbf{r},t) = F(\mathbf{r})\,\mathbf{H}_0(\mathbf{r},t) \qquad (18)$$

where $F(\mathbf{r})$ is some positive definite space function that vanishes at the limit of the computational domain. Inserting (17) and (18) in curl's Maxwell' equations (1) and (2) yields:

$$-\sigma^*\cdot\mathbf{H} - \mu\frac{\partial \mathbf{H}}{\partial t} = \nabla\wedge\mathbf{E} - \underline{\frac{1}{F}\nabla F\wedge\mathbf{E}} \qquad (19) \qquad\qquad \sigma\cdot\mathbf{E} + \varepsilon\frac{\partial \mathbf{E}}{\partial t} = \nabla\wedge\mathbf{H} - \underline{\frac{1}{F}\nabla F\wedge\mathbf{H}} \qquad (20)$$

The underlined factors can be grouped and considered as loss terms. Taking $F(\mathbf{r}) = f(x)f(y)f(z)$, one can discretize (19) and (20) and apply again the general procedure described in [8] to obtain reflected voltages for a TLM algorithm. Once the auxiliary fields are computed, true solutions are easily extracted from (17) and (18). This procedure is very attractive as it is theoretically valid for any type of waves and doesn't need computations in some extra layers like in PML techniques. In addition, it does not require extra stubs. Finally, the extra memory needed to store $F(\mathbf{r})$ is generally $2(N_x+N_y+N_z)$ wich is negligible.

III Conclusion

A class of recent ABC that can be implemented in TLM were presented. Most of the techniques are based on perfectly matched layers that surround the computational domain. The basic PML leads to two types of approaches: the split and unified algorithm. For the later, stability issues have still to be addressed. Nevertheless, good absorbing conditions can be achieved but generally inferior to the ones achieved by FDTD computations. Finally, two recent techniques implemented in the TLM algorithm were proposed. Again, stability issues must be addressed. However, the condensed nature of the TLM scheme may bring some potential advantage in the TAB technique, for instance, as compared to FDTD.

References

[1] Bérenger J.-P., "A perfectly matched layer for the absorption of electromagnetic waves", *J. Comput. Phys.*, vol. 114, n° 2, pp. 110 117, 1994.

[2] Gedney S.D., " Anisotropic perfectly matched layer-absorbing medium for the truncation of FDTD lattices", *IEEE Trans. Ant. and Prop.*, vol. 44, no°12, pp. 1630-1639, 1996.

[3] Peng J. and Balanis A., "Transparent Absorbing Boundary (TAB) for Truncation of the Computational Domain", *IEEE Microwave and Guided Wave Letters*, vol. 7, n° 10, pp. 347-349, 1997.

[4] Eswarappa Ch. and Hoefer W.J.R., "Implementation of Bérenger's absorbing boundary conditions in TLM by interfacing FDTD perfectly matched layers", *Electronics Letters*, vol. 31, no. 15, pp. 1264-1266, 1995.

[5] Peña N. and Ney M., "A New TLM Node for Bérenger's Perfectly Matched Layer", *IEEE Microwave and Guided Wave Letters*, vol. 6, n° 11, pp. 410 412, 1996.

[6] N. Penã and M. M. Ney, " Absorbing Boundary Conditions Using Perfectly Matched Layer (PML) Technique for Three-Dimensional TLM Simulations", *IEEE Trans. Microwave Theory Tech.*, vol. 45, no°10, 1997.

[7] Trenkic V., "Efficient Computation Algorithms for TLM". *First Int. Workshop on TLM Modeling*, Victoria, pp. 77 80, 1995

[8] N. Peña and M. M. Ney, "A General Formulation of a Three - dimensional TLM Condensed Node with the Modeling of Electric and Magnetic Losses and Current Sources", *12th Annual Review of Progress in Applied Computational Electromagnetics (ACES)*, Monterey, March 18-22, pp. 262-269, 1996.

[9] S. Le Maguer, N. Penã and M. M. Ney, " Matched absorbing medium techniques for full-wave TLM simulation of microwave and millimeter-wave components", *Annales Télécom.*, vol. 53, no. 3-4, 1998

[10] Dubard J.L. and Pompei D., "Efficiency of the new TLM-PML Node". *Second Int. Workshop on TLM Modeling*, München, Germany, pp. 103-111, 1997.

[11] Paul J, Christopoulos and Thomas D.W.P., "Perfectly matched layer for transmission line modelling (TLM) method", *Electronics Letters*, vol. 33, no. 9, pp. 729-730, 1997.